Distinct Dependence Of Flame Speed To Stretch And Curvature

F. Thiesset[1], F. Halter[1], C. Bariki[1], C. Chauveau[1], I. Gökalp[1]
[1] CNRS ICARE, Avenue de la Recherche Scientifique, 45072 Orléans Cedex 2 France

1 Introduction

The flamelet hypothesis requires closure equations providing an explicit relation between the flame geometrical properties (flame surface, stretch, curvature, etc) and the flame kinematic features (flame displacement and/or consumption speeds). In this prospect, asymptotic theories [1, 2] have highlighted that the flame displacement speed S_d and consumption speed S_c should vary linearly with respect to flame stretch K, i.e. the relative increase in flame surface, viz.

$$S_{c,d} = S_l^0 - K\mathcal{L}_{c,d} = S_l^0 - (K_T + K_C)\,\mathcal{L}_{c,d} \tag{1}$$

where S_l^0 is the flame propagation speed of an unstretched planar flame. The flame stretch K can be decomposed into two contributions, i.e. $K = K_T + K_C$, one due to tangential strain $K_T = -\boldsymbol{nn} : \boldsymbol{\nabla u} + \boldsymbol{\nabla} \cdot \boldsymbol{u}$ and the other one to the flame propagative/curved character $K_C = 2S_d\kappa_m$. The curvature κ_m is defined as the average of the two principal curvatures κ_1 and κ_2. $\mathcal{L}$ has the dimension of a length-scale and is referred to as the Markstein length [3]. The ratio of the Markstein length to the flame thickness l_f is called the Markstein number $\mathcal{M}$ [3]. l_f is defined by D_{th}/S_l^0, with D_{th} the thermal diffusivity.

Later, [4] noticed that Eq. (1) is not generic since it is not invariant by surface change within the flame thickness. When considering the finite thickness of the preheat zone, asymptotic theories [2] have indicated that

- the flame displacement speed is unequally altered by stretch and curvature so that two distinct Markstein lengths should be used: one characterizing the dependence of the displacement speed to stretch (referred to as the stretch Markstein length $\mathcal{L}_K$), and the other to curvature (the curvature Markstein length $\mathcal{L}_\kappa$). This decomposition was originally proposed by [4] on the basis of a phenomenological analysis.
- the Markstein number depends on the particular iso-level used to track the flame.

The displacement speed at a given isotherm now writes

$$\widetilde{S_d}(\theta) = S_l^0 - \mathcal{L}_K(\theta)K - \mathcal{L}_\kappa(\theta)2S_l^0\kappa_m \quad (2)$$

where $\widetilde{S_d}$ is the density weighted displacement speed, i.e. $\widetilde{S_d} = \rho S_d/\rho_u$ at a given isotherm $\theta = T/T_u$. Eq. (2) indicates that in an unstretched curved flame (as in the case of a stationary spherical flame), S_d is different from S_l^0. This implies that stretch is not the only scalar quantity affecting the flames kinematic properties. Therefore one has to assess and distinguish the relative contributions of curvature and strain in the evolution of S_d (and possibly S_c). This is not possible in a spherically expanding flame as curvature and strain are proportional to each other, and it is not either in a counter-flow flame configuration since curvature is not present. [5] have also shown that the stretch and curvature Markstein numbers strongly vary in the vicinity of the unburned gases whereas when travelling towards the burned gases, $\mathcal{L}_K$ tends to a plateau while $\mathcal{L}_\kappa$ goes to zero. Functional expressions for $\mathcal{L}_\kappa$ and $\mathcal{L}_K$ also reveal $\mathcal{L}_\kappa$ dominates over $\mathcal{L}_K$ when the iso-therm used to track the flame is close to the unburned gas. [2, 5] also indicated that the curvature Markstein length $\mathcal{L}_\kappa$ is independent of the type of fuel whereas $\mathcal{L}_K$ depends on the effective Lewis number.

In the present paper, focus is shed on the dependence of the flame kinematic properties (flame displacement and consumption speed) to stretch, curvature and strain. The main target is to address whether or not flame stretch is the only geometrical scalar affecting the flame speed. If not, is the Two Markstein Numbers Theory (abbreviated TMNT) proposed by [2,4] appropriate? Our configuration is a flame interacting with a vortex which contrary to spherically expanding or counter flow flames allow stretch and curvature effects to be independently studied. For measuring $\langle S_d \rangle$ and $\langle S_c \rangle$ (the area weighted displacement and consumption speeds), we use the integral method presented at the same conference in a paper entitled *"Experimental assessment of the displacement and consumption speeds in flame/vortex interactions"* by Thiesset et al. The reader is referred to the aforementioned paper for further details.

2 Experimental setup

Experiments have been carried out in the so-called Flame/Vortex Interaction Burner (FVIB, Fig. 1) developed at ICARE, Orléans France. It is a stagnation point flame burner supplemented by a vortex generator which allow to create toroidal vortices which travels trough the burner and then interact with the flame. The burner and measuring technique have been fully described in [6] and is only briefly recalled here.

Fuel and oxidizer are mixed before being fed through the side of the burner. The reactive mixture then flows into the burner plenum through a 5 mm thick aluminium grid whose role is to prevent turbulent structures to be convected in the burner. A contraction ending with a 15 mm diameter is used to create a nearly top hat velocity profile with low turbulent intensity at the burner exit. The burner-to-stagnation plate distance is 25 mm and the outlet velocity of reactive mixture is such that the flame is stabilized approximatively 10 mm downstream the burner outlet, i.e. 15 mm upstream the stagnation plate. This allows to investigate FVIs without being affected by any wall effects. This large burner-to-stagnation plate distance also allows to minimise the tangential strain rate at steady state before interaction with the vortex. To avoid external perturbations and improve flame stability, a laminar coaxial shroud of nitrogen is used. The exit co-flow velocity is $0.1\ \mathrm{m.s}^{-1}$. We have investigated a stoichiometric methane/air mixture and a lean ($\phi = 0.9$) propane/air mixture. Only results of stoichiometric methane/air mixtures will be described in the present paper.

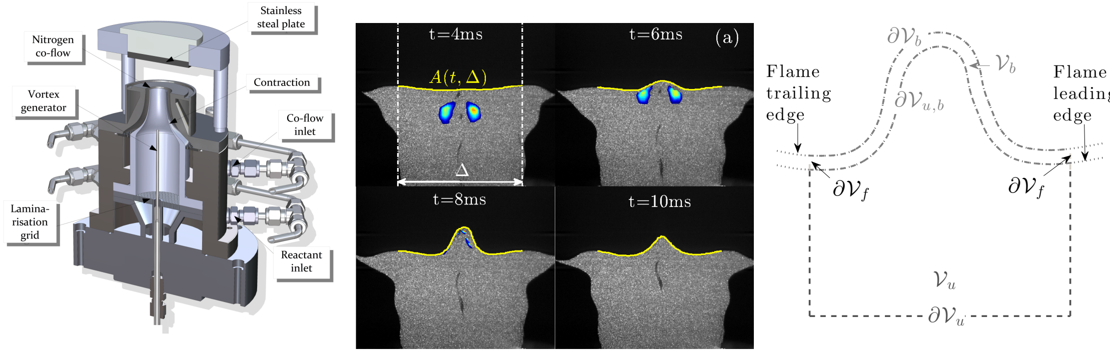

Figure 1: (left) Schematic of the Flame-Vortex Interaction Burner (FVIB). (center) Time sequence of vorticity contours superimposed on the raw Mie scattering image together with the flame location. Δ is the diameter of the cylindrical control volume over which the mass budget is calculated. (right) Control volume over which the fuel mass fraction is integrated to yield measurable expressions for the displacement and consumption speeds

The toroidal vortex generator consists of a tube of 2mm in diameter located on the centreline, 35 mm upstream the burner outlet (Fig. 1). This tube is connected to a pressurized tank located upstream. The vortex is generated by applying a sudden pressure discharge of reactive mixture at the same equivalence ratio as the main flow. The intensity of the vortex is controlled by varying the pressure magnitude within the pressurized tank. To control the duration of the pressure discharge, we use two electro-valves [6].

Flame front positions and velocity fields are simultaneously measured by means of Mie scattering laser tomography and Particle Image Velocimetry (PIV). The flow is seeded with Di-Ethyl-Hexyl-Sebacate (DEHS) droplets supplied by an atomizer. Typical size of droplets is about 1μm. The light source is a continuous Coherent Verdi G20 Laser which can deliver up to 20W at 532nm. A laser power of 2.5W was sufficient in the present case. The light scattered by the droplets is captured by a Phantom V1611 camera, equipped with a Sigma EX 180mm 1:2.8 Macro, working at an acquisition rate of 21000Hz with a field of view of 896$\times$800 pixels^2. The spatial resolution is 36.72px/mm. Typical records of a flame/vortex interaction is presented in Fig. 1 (center). One observes that at a time t=4ms (time t=0 was arbitrary set to the time when the vortex center is at x=2.5mm above the burner exit), the flame is rather flat suggesting that the vortex generator is sufficiently far from the burner outlet for not creating a wake. As the vortex is convected (t=6ms and 8ms), the flame is increasingly stretched. Its area then reaches a maximum before decreasing (t=10ms) while the flame goes back to its original position.

The experimental database covers the range $0.5 < U_\theta/S_l^0 < 3$ whereas R_v/δ_{th} slightly varies around 7. S_l^0 is the unstretched laminar flame speed, δ_{th} is the thermal flame thickness based on the maximum temperature gradient. U_θ and R_v are the vortex rotational velocity and the vortex core-to-core distance, respectively.

3 Results

The derivations of the displacement and consumption speeds are fully provided in [7]. Only the main results are recalled here. As shown in [7], the area weighted displacement speed $\langle S_d^u \rangle$ can be estimated from the integrated fuel mass fraction and writes

$$\langle S_d^u \rangle = -\frac{1}{A_f}\frac{\mathrm{d}\mathcal{V}_u}{\mathrm{d}t} - \frac{1}{A_f}\oint_{\partial\mathcal{V}_u(t)} \boldsymbol{u}\cdot\boldsymbol{n}\mathrm{d}^2A \tag{3}$$

where $\mathcal{V}_u$ is the unburned gases volume comprised within the boundaries $\partial\mathcal{V}_u + \partial\mathcal{V}_{u,b}$. A_f is the flame surface. A_f and $\mathcal{V}_u$ (together with the mean curvature κ_m) are estimated from 2D images thanks to axisymmetry. $\boldsymbol{u}\cdot\boldsymbol{n}$ is the normal flow velocity at the boundary $\partial\mathcal{V}_u$ where $\boldsymbol{n}$ is the outwardly pointing normal vector (Fig. 1). Note that the superscript u has been kept for designating S_d^u as it corresponds to the displacement speed at (close to) the leading edge $\partial\mathcal{V}_{u,b}$. Integrating the fuel mass fraction transport equation over the "flame" volume which is comprised between the boundaries $\partial\mathcal{V}_{u,b}$, $\partial\mathcal{V}_b$ and $\partial\mathcal{V}_f$ leads to an expression for the area weighted fuel consumption speed $\langle S_c \rangle$

$$\langle S_c \rangle = \langle S_d^u \rangle - \mathcal{F}\left(\frac{1}{A_f}\frac{\mathrm{d}A_f}{\mathrm{d}t} + \frac{1}{A_f}\pi\Delta v_r\right) \tag{4}$$

where $\mathcal{F} = \delta_L/2$ [7] (δ_L is the thermal flame thickness), Δ is the diameter of the control volume, and v_r is the tangential velocity at the junction between $\partial\mathcal{V}_u$ and $\partial\mathcal{V}_f$.

The evolution of $\langle S_d^u \rangle$ and $\langle S_c \rangle$ during a flame/vortex interaction is studied as a function of the area weighted stretch rate $\langle K \rangle = \mathrm{d}(\log A_f)/\mathrm{d}t$, the area weighted curvature contribution to stretch $\langle K_C \rangle = \langle 2S_d^u\kappa_m \rangle$ and the area weighted tangential strain rate $\langle K_T \rangle = \langle K \rangle - \langle K_C \rangle$. Results are presented in Fig. 2. For the sake of clarity we consider only the methane/air flame at $U_\theta/\langle S_c^1 \rangle = 2.8$ (U_θ being the vortex rotational velocity) but similar trends were observed for propane/air flames and different vortex intensities. Different widths Δ of the control volume are considered in Fig. 2 in order to emphasize that the trends in the data are the same irrespectively of Δ. Quantitatively, it is straightforward that due to averaging, the larger Δ, the smaller the variations of $\langle S_d^u \rangle$, $\langle K \rangle$, $\langle K_T \rangle$ and $\langle K_C \rangle$. This is what is observed in Fig. 2.

Before $\langle K \rangle$ reaches its maximum value, $\langle S_d^u \rangle$ increases almost linearly with $\langle K \rangle$ (Fig. 2(a)). However, if Eq. (1) were to apply, $\langle S_d^u \rangle$ should have been decreasing towards its original value following the decrease of $\langle K \rangle$. This trend is not observed since $\langle S_d^u \rangle$ continues to increase while the stretch decreases. This confirms that another phenomenon than stretch is at play and that the Eq. (1) does not apply in a Flame/Vortex Interaction.

When plotted against $\langle K_C \rangle$ (Fig. 2(b)), the displacement speed appears to be nicely correlated with flame curvature. Here $\langle S_d^u \rangle$ is represented as a function of $\langle K_C \rangle$ the propagation/curvature contribution to stretch but a similar (if not better) correlation was found with $\langle \kappa_m \rangle$. The correlation $\langle S_d^u \rangle$ versus $\langle \kappa_m \rangle$ is almost linear and the slope is found to be marginally dependent on the Lewis number (not shown). $\langle S_d^u \rangle$ is also represented as a function of tangential strain $\langle K_T \rangle$ in Fig. 2(c). $\langle S_d^u \rangle$ first follows nicely the increase of $\langle K_T \rangle$. Then, $\langle S_d^u \rangle$ has a sort of S-shape evolution with respect to $\langle K_T \rangle$ meaning that $\langle S_d^u \rangle$ is not uniquely correlated to $\langle K_T \rangle$ neither. As a conclusion, Eq. (1) is not applicable to FVI since the correlation between $\langle S_d^u \rangle$ and $\langle K \rangle$ is not bijective. Another geometrical scalar than stretch is at play. Our data suggests that curvature could be this leading-order parameter in agreement with Eq. (2). To confirm this, we now provide comparisons between our data and the predictions of the TMNT (Eq. (2)). Applying surface averaging to Eq. (2) yields

$$\langle S_d^u \rangle = S_l^0 - \mathcal{L}_\kappa S_l^0 2\langle \kappa_m \rangle - \mathcal{L}_K \langle K \rangle \tag{5a}$$

$$\langle S_c \rangle = S_l^0 - \mathcal{L}_\kappa 2S_l^0 \langle \kappa_m \rangle - (\mathcal{L}_K + \mathcal{F})\langle K \rangle - \mathcal{F}\frac{\pi\Delta v_r}{A_f} \tag{5b}$$

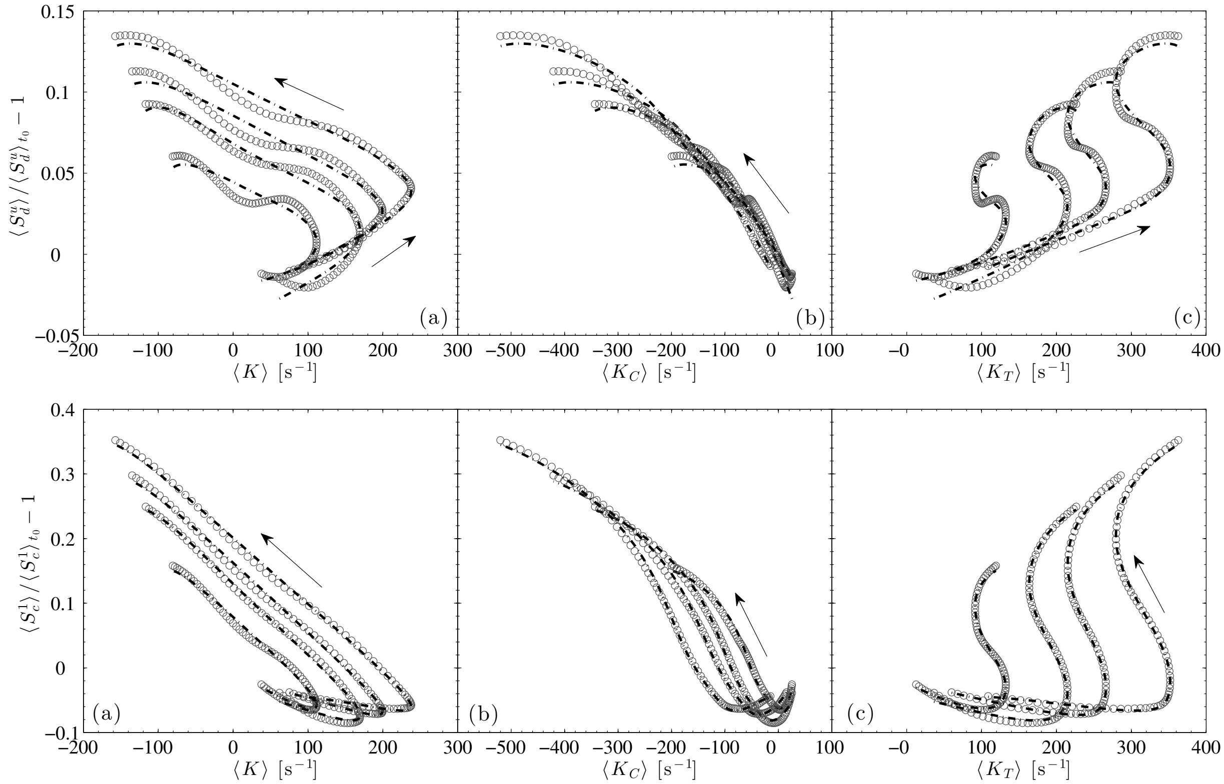

Figure 2: Plots of $\langle S_d^u \rangle$ (top) and $\langle S_c \rangle$ (bottom) versus $\langle K \rangle$ (a), $\langle K_c \rangle$ (b) and $\langle K_T \rangle$ (c) for methane/air mixture at $U_\theta / \langle S_c^1 \rangle_{t_0} = 2.8$. The arrow indicates the direction of increasing time. The different curves correpond to different width Δ of the control volume; the smaller Δ the larger the variations of $\langle S_d^u \rangle$, $\langle S_c \rangle$, $\langle K \rangle$, $\langle K_C \rangle$ and $\langle K_T \rangle$. The dotted lines correponds to predictions using Eqs. (5a) and (5b) with $\mathcal{L}_\kappa = 4.98 l_f$ and $\mathcal{L}_K = -1.08 l_f$

By fitting to experimental data, $\mathcal{L}_\kappa$ and $\mathcal{L}_K$ (together with S_l^0) can be estimated to $4.98 l_f$ and $-1.08 l_f$, respectively. With these values, the measured evolution of $\langle S_d^u \rangle$ and $\langle S_c \rangle$ with respect to $\langle K \rangle$, $\langle K_C \rangle$ and $\langle K_T \rangle$ is very nicely reproduced by either Eq. (5a) or Eq. (5b) (dashed curves in Fig. 2). This is the main result of the present study as it provides unprecedented quantitative support for the two Markstein numbers approach. For propane flames, similar agreement was observed with $\mathcal{L}_\kappa = 5.12 l_f$ and $\mathcal{L}_K = -0.25 l_f$. Our data are thus consistent with the TMNT since $\mathcal{L}_\kappa$ is almost independent of Le while $\mathcal{L}_K$ is clearly different between methane and propane flames. Furthermore, as the displacement speed is here measured close to the unburned gases, $\mathcal{L}_\kappa$ dominates over $\mathcal{L}_K$ consistently with the TMNT. These results were rather robust and independent of the vortex strengths.

4 Conclusions

This study presents a detailed experimental analysis of the relationship between kinematic and geometric properties of a premixed flame interacting with an isolated toroïdal vortex. Particular attention is paid to the influence of stretch, strain and curvature on the displacement and consumption speeds.

It is shown that flame stretch is not the only scalar geometrical quantity influencing the flame kinematic features. Indeed, curvature has a strong if not dominant contribution. This thus precludes using Eq. (1) to describe the evolution of flame speeds in wrinkled stretched flames.

Results are interpreted in the light of the TMNT [2, 4, 5]. These theories indicate that, when considering the flame structure, i.e. in the finite flame thickness case, the displacement speed strongly depends on the isotherm chosen to track the flame, and that different isotherms are not equally sensitive to stretch and curvature. Two distinct Markstein lengths are needed, one characterizing the dependence of S_d to stretch, another to curvature, and functional expressions for the two Markstein numbers were derived analytically. Up to now, the existence of the curvature Markstein numbers has been confirmed only in the very ideal case of a stationary spherical flame [5]. To the best of our knowledge, the co-existence of the two Markstein numbers has never been confirmed experimentally and no attempt was made to measure them simultaneously. This gap is bridged in the present study and provides unprecedented quantitative support for the two Markstein numbers approach.

As an overall conclusion, we may finally insist on the relevance of the flame/vortex interaction configuration. Indeed, this configuration demonstrates the relevance of the TMNT in a more realistic configuration than that of a stationary spherical flame and also highlights the feasibility of measuring simultaneously the two Markstein numbers together with S_l^0. This would not have been possible in spherically expanding flames as strain and curvature are proportional to each other or in counter-flow flames since curvature is zero. Such estimations would have been also particularly tenuous in turbulent flames notwithstanding the inherently stochastic nature of turbulence.

References

[1] P. Clavin and P. J. Garcia, "The influence of the temperature dependence on the dynamics of flame fronts," *J. Mecanique Théorique et Appliquée*, vol. 2, pp. 245–263, 1983.

[2] J. Bechtold and M. Matalon, "The dependence of the markstein length on stoichiometry," *Combust. Flame*, vol. 127, no. 1, pp. 1906–1913, 2001.

[3] G. H. Markstein, *Nonsteady flame propagation:*, vol. 75. Elsevier, 1964.

[4] P. Clavin and G. Joulin, "Flamelet library for turbulent wrinkled flames," in *Turbulent Reactive Flows*, vol. 40 of *Lecture Notes in Engineering*, pp. 213–240, Springer, 1989.

[5] G. Giannakopoulos, A. Gatzoulis, C. E. Frouzakis, M. Matalon, and A. G. Tomboulides, "Consistent definitions of flame displacement speed and markstein length for premixed flame propagation," *Combust. Flame*, vol. 162, no. 4, pp. 1249–1264, 2015.

[6] F. Thiesset, G. Maurice, F. Halter, N. Mazellier, C. Chauveau, and I. Gökalp, "Flame-vortex interaction: Effect of residence time and formulation of a new efficiency function," *Proc. Combust. Inst.*, vol. in press, 2017.

[7] F. Thiesset, F. Halter, C. Bariki, C. Lapeyre, C. Chauveau, I. Gokalp, L. Selle, and T. Poinsot, "Experimental assessment of the displacement and consumption speeds in flame/vortex interactions," *ICDERS*, vol. Boston, 2017.